



The influence of water-based nanolubrication on mill load and friction during hot rolling of 304 stainless steel

Hui Wu¹ · Dongbin Wei² · Ay Ching Hee³ · Shuiquan Huang⁴ · Zhao Xing⁵ · Sihai Jiao⁵ · Han Huang⁴ · Zhengyi Jiang¹

Received: 13 April 2022 / Accepted: 28 July 2022 / Published online: 4 August 2022
© The Author(s) 2022

Abstract

Using pure water in comparison to water-based lubricant containing 4% TiO₂ nanoparticles (NPs), the hot rolling tests of 304 stainless steel were carried out at a rolling temperature of 1050 °C under varying rolling reductions and speeds. The effects of lubrication on rolling force, torque, power and contact friction were systematically investigated. The coefficient of friction (COF) during steady-state hot steel rolling was inversely calculated using a developed flow stress model. The COF models including the effects of rolling reduction and speed were proposed via multiple linear regression. The results indicated that the use of the nanolubricant enabled a reduction of rolling force up to 6.1% and decreases in rolling torque and power up to 21.6%, compared to that of water condition. The results obtained from the linear regression agreed well with those from the inverse calculation, suggesting the developed COF models had high accuracy. The lubrication mechanisms were derived from a boundary lubrication regime, owing to ball bearing and mending effects of TiO₂ NPs, and formation of thin lubricant film under high rolling pressure.

Keywords Stainless steel · Hot rolling · Water-based nanolubricant · Coefficient of friction

1 Introduction

Hot rolling is a metalworking process extensively applied in steel manufacturing to produce a final product or a basic material for downstream processing [1]. In hot steel rolling,

rolling temperatures normally range from 800 to 1050 °C, depending on the material being rolled [2]. Stainless steels, in particular, are usually hot rolled at temperatures above 1000 °C, which aims to enhance the resistance to sticking on work roll surface [3, 4]. Such high rolling temperatures significantly expedite the degradation of work rolls in the form of oxidation and wear. There also exists a challenge to enhance the capacity of rolling mill and lower its energy consumption by reducing the mill load, especially for rolling heavy plates with high rolling reductions. Hot rolling with high reductions is also one of the most commonly used techniques to produce ultra-fine-grained steels. Therefore, a coolant and/or lubricant is needed to wet/lubricate the work roll surface during hot rolling process. Over the past decades, conventional oil lubricants such as neat oils and oil-in-water (O/W) emulsions have been widely used in hot steel rolling for reduced mill load [5], reduced work roll wear [6], thinned oxide scale and improved strip surface quality [7], controlled strip thickness [8], ameliorated flatness [9], refined grains [10], and optimised recrystallization texture [11]. Nevertheless, oil lubricants usually contain a high concentration of oil to ensure sufficient lubricity which is in fact weakened when oil is burning at high rolling temperatures. Burning

✉ Hui Wu
hwu@uow.edu.au

✉ Han Huang
han.huang@uq.edu.au

✉ Zhengyi Jiang
jiang@uow.edu.au

¹ School of Mechanical, Materials, Mechatronic and Biomedical Engineering, University of Wollongong, Wollongong, NSW 2522, Australia

² School of Mechanical and Mechatronic Engineering, University of Technology Sydney, Ultimo, NSW 2007, Australia

³ School of Chemical Engineering and Advanced Materials, The University of Adelaide, Adelaide, SA 5005, Australia

⁴ School of Mechanical and Mining Engineering, The University of Queensland, Brisbane, QLD 4072, Australia

⁵ Baosteel Research Institute (R&D Centre), Baoshan Iron & Steel Co., Ltd, Shanghai 200431, China

of oil lubricants causes environmental issues. Their disposal has the same concern owing to the non-biodegradable nature and inherent toxicity of oil [12]. To enhance the lubricity of oil lubricants but reduce the oil usage for environmental protection, nanoadditives are added into the O/W emulsions that have a low oil content [13–15]. By doing this, encouraging results have been obtained in improving the lubrication performance and mitigating the pollution problems compared with conventional oil lubricants. The use of oil-containing lubricants, however, unavoidably has adverse effects on the environment and the regular maintenance of nozzles and pipes. It is thus essential to develop eco-friendly and high-performance lubricants that can be employed in hot steel rolling even at temperatures above 1000 °C.

In recent years, water-based nanolubricants have attracted increasing attention and interest in many engineering fields such as metal machining [16–18], micro rolling [19] and other tribological applications [20–22]. These lubricants containing TiO₂ NPs [23–26], Eu-doped CaWO₄ NPs [27] or MoS₂-Al₂O₃ nanocomposites [28, 29] applied in hot steel rolling have become increasingly prevalent due to their good environmental compatibility, high recyclability, superb cooling capacity and excellent lubricity at high temperatures. The nanoadditives for synthesising water-based lubricants include pure metals, metal and non-metal oxides, metal sulphides, carbides, nitrides, carbon-based materials and composites [30]. Among all the candidates of aqueous nanoadditives, nano-TiO₂ has gained popularity in the syntheses of water-based nanolubricants on account of their low cost and exceptional dispersion stability in water [31–33]. Applying such lubricants containing TiO₂ NPs in hot steel rolling has demonstrated great potential in reducing rolling force, alleviating roll wear, decreasing oxide scale thickness, improving strip surface quality, and refining grains in rolled steels [34]. A recent study also showed that such water-based nanolubricants could be synthesised in a facile process with a super low operating cost, which sheds some light on industrial-scale hot steel rolling [35]. However, the effects of rolling parameters on the mill load using water-based nanolubricants have been scarcely reported.

When developing the water-based nanolubricants for hot steel rolling, it is imperative to investigate the contact friction between the work roll and the workpiece. The main reason behind this is that friction is of paramount importance for accurate modelling, optimal design and control of industrial rolling processes [36]. In some previous studies, the friction in hot rolling was investigated through characterising the relations between coefficient of friction (COF) and rolling parameters under dry [37, 38] or oil lubrication conditions [5, 39]. Nevertheless, the friction associated with hot rolling of steels using water-based nanolubrication remains not well understood likely due to the difficulty in measuring the COF.

This study aimed to investigate the effects of different rolling parameters on the mill load and friction during hot rolling of 304 stainless steel. The optimal water-based nanolubricant ascertained in our previous study [35] was utilised to have a comparison with pure water in this matter. The lubrication mechanisms associated with the hot rolling process were unveiled based on the lubrication regime determined through a lubricant film thickness model. New COF models of hot steel rolling were developed and validated using the rolling test results.

2 Materials and methods

2.1 Materials

Water-based nanolubricants used in this study consist of low-cost rutile TiO₂ NPs (~300 nm in diameter), and chemical additives including glycerol, sodium dodecyl benzene sulfonate (SDBS) and Snailcool. Rutile is the most stable polymorph of TiO₂ at temperatures up to its melting point of 1843 °C, and it can be irreversibly converted from metastable phases of anatase or brookite upon being heated above temperatures ranging from 600 to 800 °C [40, 41]. Glycerol is a colourless, odourless and viscous liquid that assists in enhancing viscosity and wettability of the lubricants [25]. SDBS is an organic dispersant that has a linear structure with a hydrophilic group, which helps improve the wettability, dispersion stability and viscosity of the water-based lubricants [23]. Snailcool is a novel water-soluble extreme pressure agent that not only enhances the extreme pressure property of the lubricants, but also improves the lubrication performance [34]. All the chemical additives are non-toxic and biodegradable to environment. The preparation of the water-based nanolubricants is a facile process that only involves mechanical stirring without using extra ultrasonic treatment. This process helps reduce the synthesis cost of the water-based nanolubricants, which is of particular significance for industrial application. According to the results obtained in our previous study [35], all the water-based nanolubricants with varying constituents exhibited excellent dispersion stability within 48 h. In this study, only the lubricant with the best lubrication performance was selected to compare with pure water which is a commonly used coolant for industrial-scale work rolls. The specific chemical composition of the optimal lubricant in weight percentage includes TiO₂ 4.0%, glycerol 10.0%, SDBS 0.2% and Snailcool 1.0%.

A 304 austenitic stainless steel was hot rolled in this study. Its main chemical composition in weight percentage includes C 0.047%, Si 0.51%, Mn 1.13%, Cr 18.09%, Ni 8.45%, Cu 0.046%, V 0.12%, N 0.027 and P 0.027%. The steel workpieces were machined to 300 ± 0.5 mm in

length, 48 ± 0.3 mm in width and 10.8 ± 0.1 mm in thickness with tapered edges for ease of biting. Both sides of the workpieces were ground to achieve a consistent surface roughness (R_a) of around $0.5 \mu\text{m}$. The workpieces were then cleaned with acetone to remove any residues retained from machining.

2.2 Hot rolling test

Hot rolling tests were carried out on a 2-high Hille 100 experimental rolling mill. The work roll diameter and the roll barrel length were 225 and 254 mm, respectively. The initial surface roughness of work rolls was $0.9 \mu\text{m}$ in R_a . During testing, the steel workpieces were first reheated in a high-temperature electric resistance furnace at 1100°C and then soaked for 40 min in a nitrogen atmosphere. The actual rolling temperature was about 50°C lower than the reheating temperature. As shown in Table 1, the rolling reduction ranged from ~10 to ~30%, and the rolling speed was in the range of 10–50 rpm, i.e. $0.12\text{--}0.6 \text{ m}\cdot\text{s}^{-1}$. The hot rolled strips were immediately put into a cooling box inflated with nitrogen to restrain further oxidation. As reported elsewhere [26], prior to each rolling test, the lubricant was continuously sprayed onto the pre-cleaned rotating work rolls until supersaturated coverage was achieved. The hot steel rolling under the same testing condition was repeated twice to attain average data of rolling force, torque and power.

2.3 Flow stress model for inverse calculation of COF

The COF during steady-state hot rolling of 304 stainless steel was acquired using a numerical model developed by Alexander based on the Orowan rolling model [42, 43]. The Alexander model with detailed features and theory can be found elsewhere [44, 45]. In the Alexander model, the flow stress of the steel used for COF calculation is expressed as [42]:

$$\sigma = A \cdot (1 + B\varepsilon)^{n_1} \cdot (1 + D\dot{\varepsilon})^{n_2} \tag{1}$$

where $A = \sigma_0 \cdot e^{-aT}$; σ_0 is the base yield stress (MPa); T is the temperature (K); B, D, a, n_1 and n_2 are constants; ε and $\dot{\varepsilon}$ denote the strain and strain rate (s^{-1}), respectively. Assuming $B = D = 1000 \gg 1$, A, n_1 and n_2 in Eq. (1) can be determined using the multiple regression of the stress–strain curves obtained from hot compression tests. A MATLAB programme was developed based on the Alexander model to conduct the inverse calculation of COF. When running the MATLAB programme, the COF value was input and adjusted until the calculated rolling force was less than 1% error with the measured one.

The flow stress of 304 stainless steel was achieved by hot compression tests conducted on a Gleeble-3500 Thermomechanical Simulator in vacuum under 1.0×10^{-2} torr pressure at 1050°C . The compressive strain was limited up to 0.5. The strain rates being selected were 7.6 and 10.0 s^{-1} , falling into the range of strain rate in the hot rolling tests. The strain rate of hot steel rolling was calculated using the Ford-Alexander equation [46]:

$$\dot{\varepsilon} = \frac{\pi N}{30} \sqrt{r/h_0} \left(1 + \frac{\varepsilon'}{4}\right) \sqrt{\varepsilon'} \tag{2}$$

where $\dot{\varepsilon}$ is the strain rate (s^{-1}); N is the rotation speed (rpm); r is the work roll radius (mm); h_0 is the entry thickness (mm); and ε' is the rolling reduction.

2.4 Measurement and characterisation

Rolling force data during hot steel rolling were acquired through two individual transducers located at both the drive and operation sides over the bearing blocks of the top work roll. Two torque transducers were placed in the drive spindles to measure the rolling torque. The rolling speed was monitored using a tachometer, and the roll gap was precisely controlled using a rotary knob mounted on a control panel. A pyrometer was applied to measure the entry temperature. All the data were collected using a programme developed on the basis of MATLAB xPC technology [35].

Table 1 The design of hot rolling tests

Rolling temperature ($^\circ\text{C}$)	Rolling reduction	Rolling speed ($\text{m}\cdot\text{s}^{-1}$)	Lubrication condition
1050 $^\circ\text{C}$	10%	0.12	Water and 4.0 wt% TiO_2 lubricant
	10%	0.36	
	10%	0.6	
	20%	0.12	
	20%	0.36	
	20%	0.6	
	30%	0.12	
	30%	0.36	
	30%	0.6	

Surface morphologies of rolled steels were examined and analysed under a high-resolution field emission scanning electron microscope equipped with an energy-disperse spectrometer (EDS) to investigate the role of NPs during rolling process.

Dynamic viscosity values of the applied lubricants were measured at 80 °C under high pressures of 0, 50, 100 and 150 bar, i.e. 0, 5, 10 and 15 MPa, using an Anton Paar MCR 302 Rheometer. The testing temperature was chosen to avoid substantial loss of water caused by rapid evaporation at a temperature above 80 °C. By doing this, the lubricant concentration would not be affected significantly during the viscosity measurement. The shear rate used for the viscosity measurement ranged from 1 to 1000 s⁻¹. Each measurement was repeated three times, and the averaged values were obtained.

3 Results

3.1 Rolling force, torque and power

Rolling force values are plotted as a function of the rolling reduction varying from ~10 to ~30% for all the rolling speeds being used, as shown in Fig. 1. The rolling force increases with the increased rolling reduction for both water and 4% TiO₂ lubricant. The rolling force (F , kN) is linearly related to the rolling reduction (ϵ') with correlation coefficients (R^2) above 0.98, which can be expressed below.

$$F = 11.6 + 713.83\epsilon' \quad R^2 = 0.987 \text{ for water} \quad (3)$$

$$F = 13.43 + 702.25\epsilon' \quad (R^2 = 0.983) \text{ for 4\% TiO}_2 \text{ lubricant} \quad (4)$$

In comparison to water, 4% TiO₂ lubricant enables a linear function with a smaller slope, indicating that the rolling force changes less significantly with the reduction when using 4% TiO₂ lubricant instead of water. In the hot rolling of 304 stainless steel at 1050 °C, Eqs. (3) and (4) can be used to predict the rolling force values under certain rolling reductions due to their high linear correlation coefficients.

Figure 2 shows the rolling force that changes with the rolling speed under rolling reductions of 10–30% using water compared with 4% TiO₂ lubricant at the rolling temperature of 1050 °C. Under each reduction, the rolling force obtained using water or 4% TiO₂ lubricant increases with the increased rolling speed. Compared to water, 4% TiO₂ lubricant brings about much lower rolling force, especially under relatively low rolling reduction and speed. In particular, the rolling force is decreased up to 6.1% when using 4% TiO₂ lubricant under 10% rolling reduction at a rolling speed less than 0.36 m·s⁻¹. The lubrication effect on decreasing the rolling force appears to be less significant under higher rolling reduction and speed.

According to Eq. (2) and the rolling parameters listed in Table 1, the strain rate calculated in this study ranges from 1.1 to 10.1 s⁻¹. The rolling force plotted as a function of the strain rate using water and 4% TiO₂ lubricant is shown in Fig. 3. It can be seen that the rolling force changes insignificantly with the strain rate under each rolling reduction for both water and the lubricant. Besides, the linear fitting results with 4% TiO₂ lubricant are slightly better than those with water.

The rolling torque values are plotted against the rolling speed under different rolling reductions in Fig. 4. The

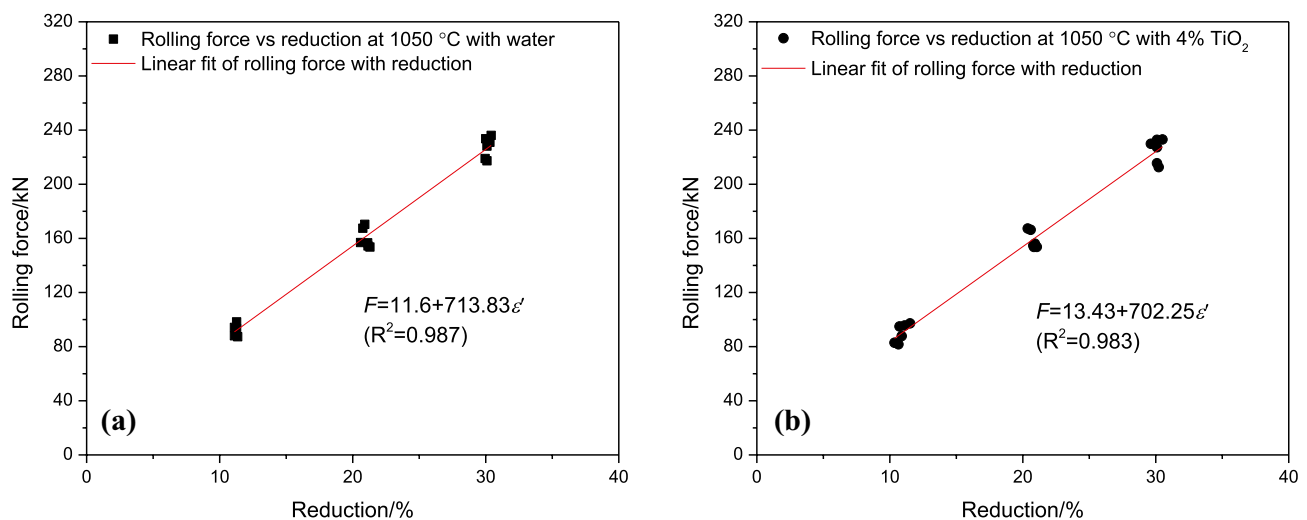


Fig. 1 Rolling force plotted as a function of rolling reduction using **a** water and **b** 4% TiO₂ lubricant at a rolling temperature of 1050 °C. Data points at each reduction indicate that different rolling speeds were used under the reduction

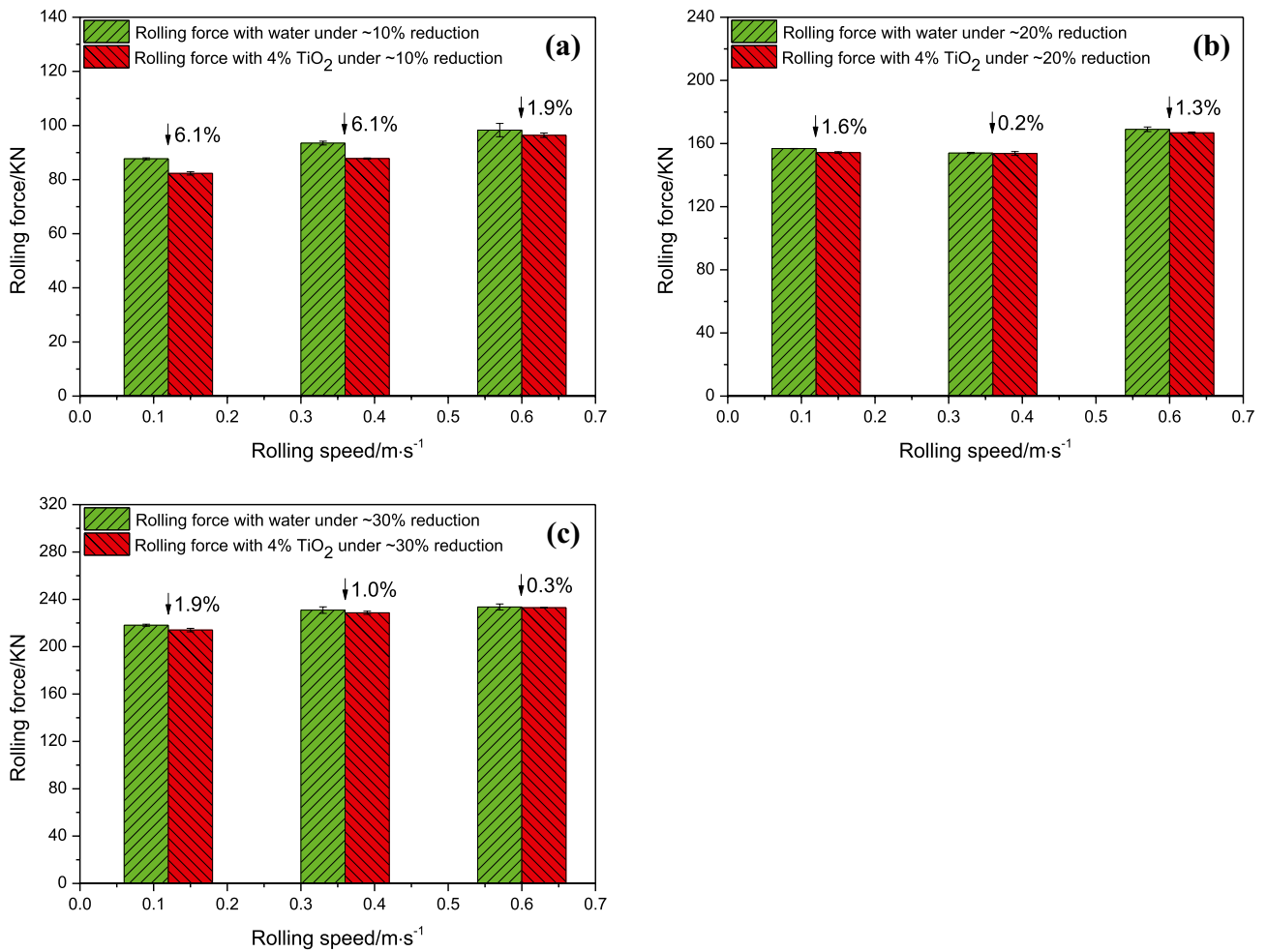


Fig. 2 Rolling force plotted against rolling speed under rolling reductions of **a** ~10%, **b** ~20% and **c** ~30% using water and 4% TiO₂ lubricant at 1050 °C

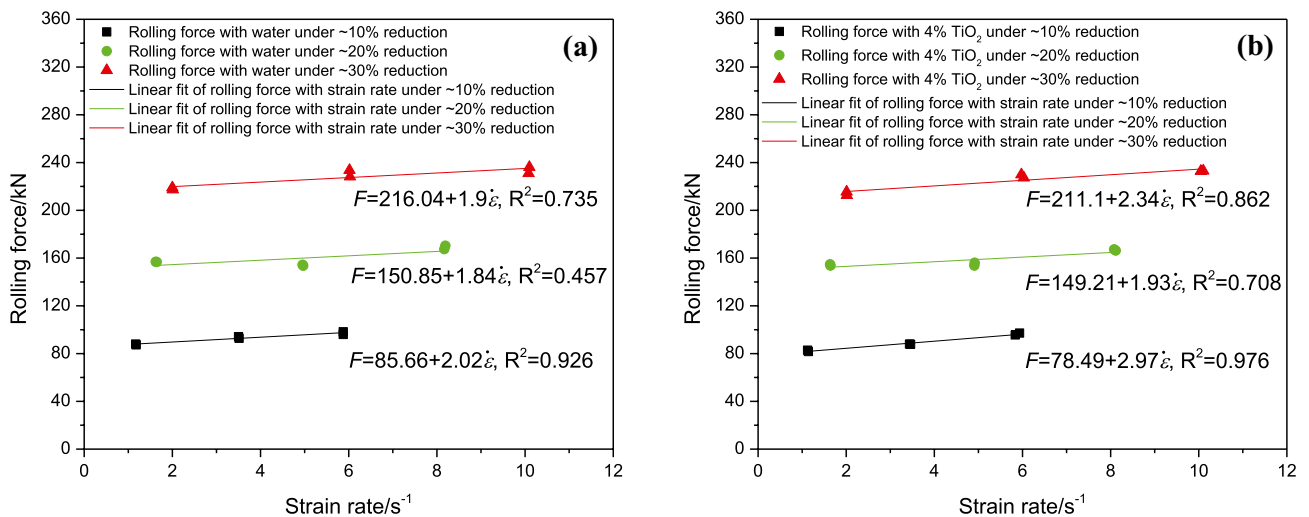


Fig. 3 Rolling force plotted as a function of strain rate using **a** water and **b** 4% TiO₂ lubricant

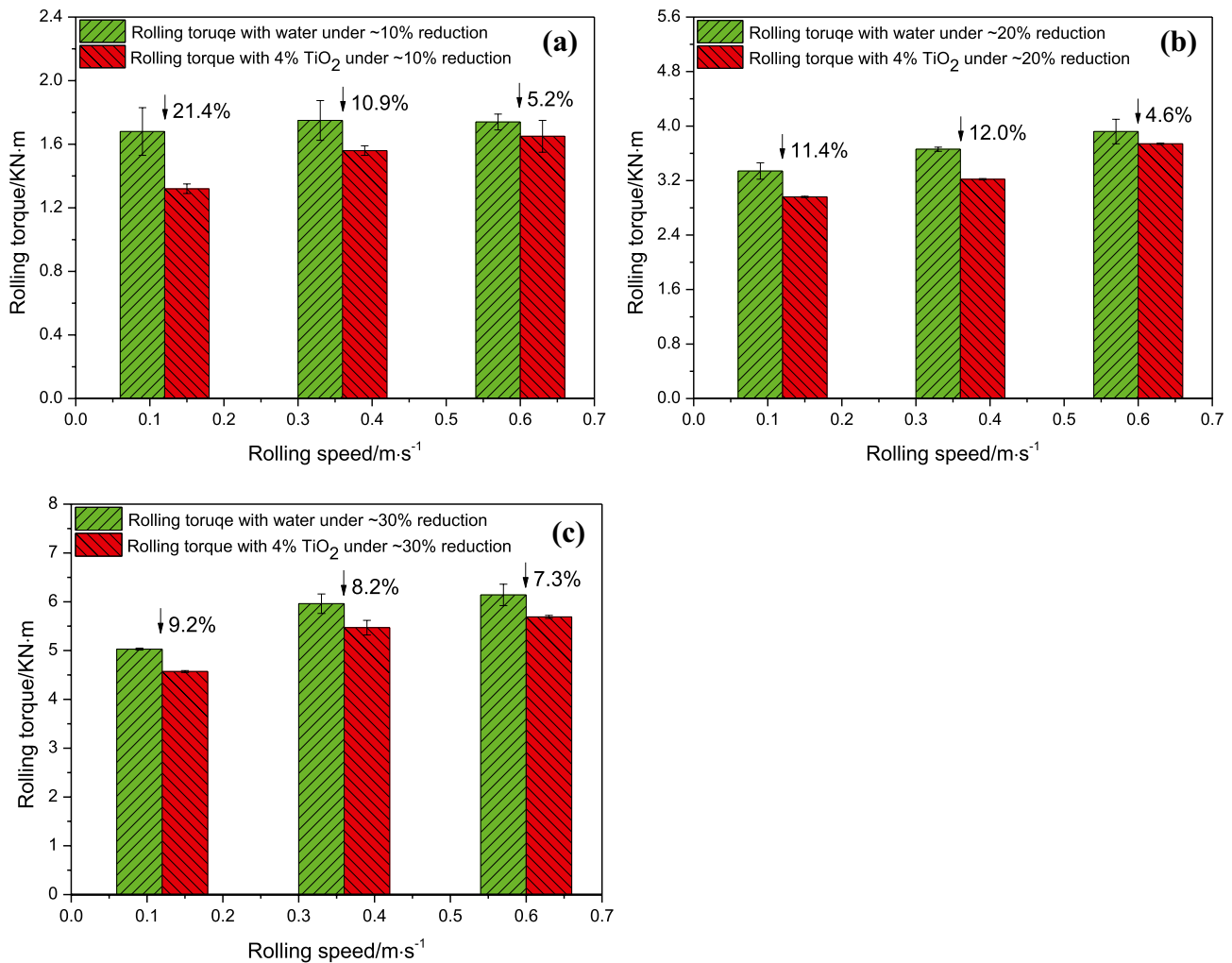


Fig. 4 Rolling torque plotted against rolling speed under reductions of **a** ~10%, **b** ~20% and **c** ~30% using water and 4% TiO₂ lubricant at 1050 °C

results show a similar variation trend to those in Fig. 2. The use of 4% TiO₂ lubricant can decrease the rolling torque obtained with water by around 5–21%, under all the rolling conditions. A slower rolling test combined with a smaller rolling reduction causes a better lubrication effect on decreasing the rolling torque.

The power applied to the rolling mill results from the torque applied to the work rolls. Rolling power is a quantity that represents the energy consumption of a rolling mill, which is calculated as:

$$P = \frac{2\pi}{60} \times M \times \omega \quad (5)$$

where P is the rolling power (kW); M is the rolling torque (kN·m); and ω is the rolling speed (rpm).

Figure 5 shows that the rolling power rises with the increased rolling speed under each reduction. The results

also show that the rolling power falls significantly by up to 21% using 4% TiO₂ lubricant. The extent of power reduction presents a descending trend with the increased rolling speed and rolling reduction, but it is generally over 5%.

3.2 Coefficient of friction

Figure 6 shows the true stress–strain curves obtained from the hot compression tests at 1050 °C with the strain rates of 7.6 and 10.0 s⁻¹. It is evident that the flow stress rises dramatically with the increase in strain, and a higher strain rate leads to a higher flow stress. The parameters in Eq. (1) are obtained from the regression result of the stress–strain curves:

$$\sigma = 10.588 \cdot (1 + 1000\varepsilon)^{0.3996} \cdot (1 + 1000\dot{\varepsilon})^{0.0772} \quad (6)$$

where σ is the stress (MPa); ε and $\dot{\varepsilon}$ represent the strain and strain rate (s⁻¹), respectively.

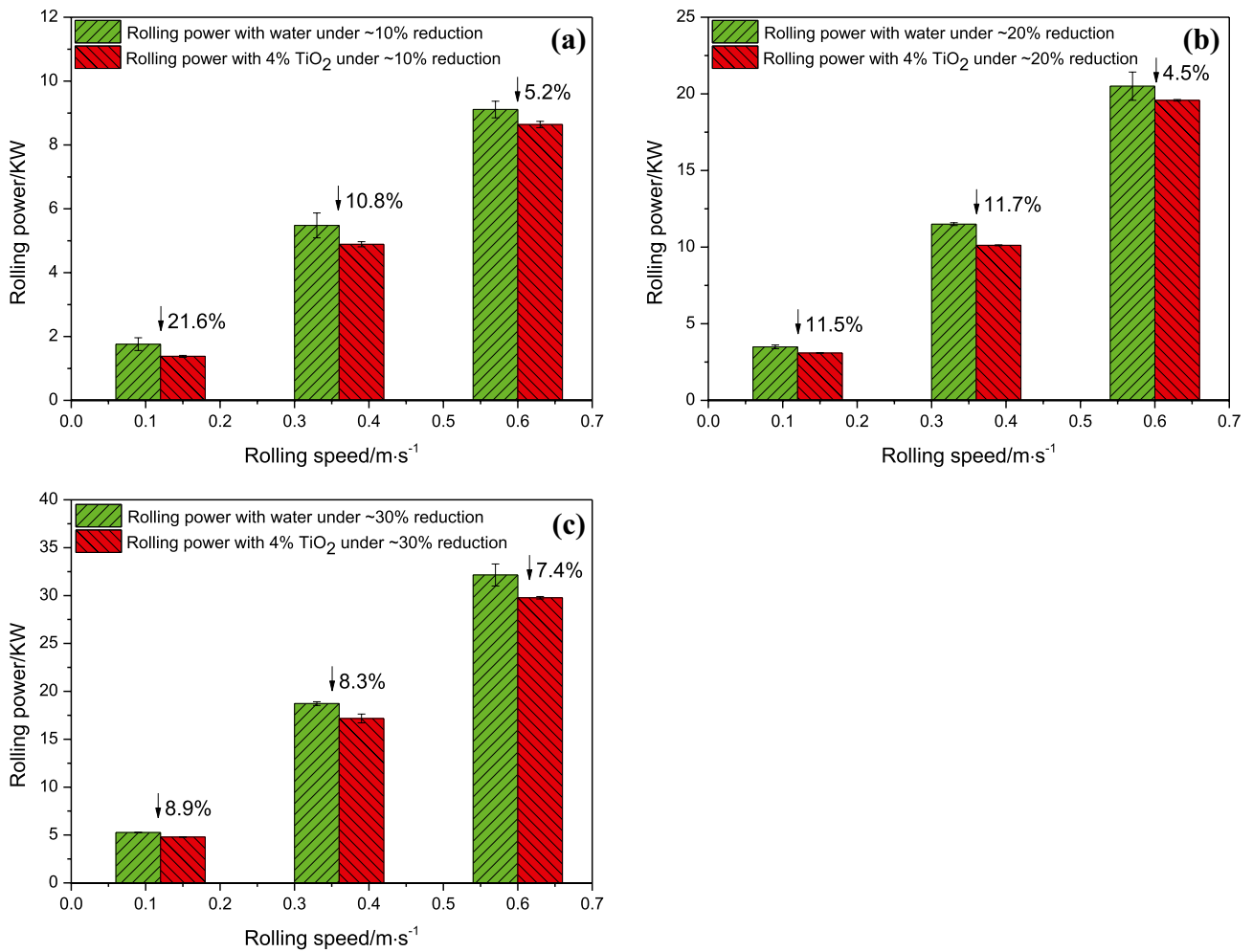


Fig. 5 Rolling power plotted against rolling speed under reductions of **a** ~10%, **b** ~20% and **c** ~30% using water and 4% TiO₂ lubricant at 1050 °C

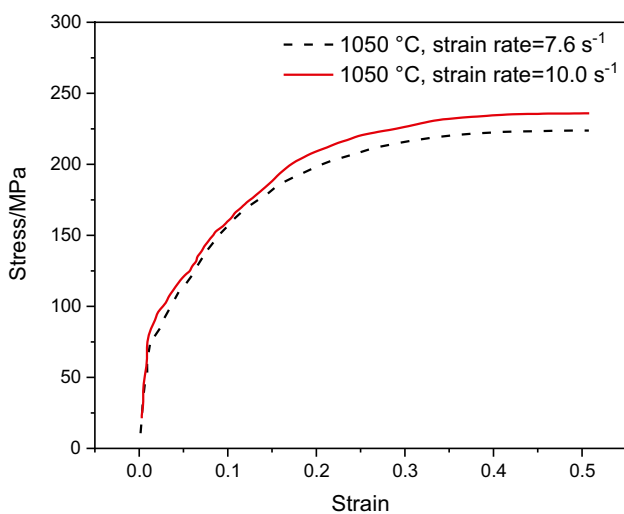


Fig. 6 True stress–strain curves of the 304 stainless steel compressed at 1050 °C using the strain rates of 7.6 and 10.0 s⁻¹

By introducing Eq. (6) into the developed MATLAB programme, the COF during steady-state hot rolling of 304 stainless steel can be calculated and is demonstrated in Table 2. It is found that the use of 4% TiO₂ lubricant results in a lower COF compared to that of water under each rolling condition. Of particular interest is that the COF can be lowered to a greater extent under the rolling reduction of ~10% combined with a rolling speed of 0.12 m•s⁻¹.

According to [47], the COF (μ) during hot steel rolling is linearly related to workpiece temperature (T , °C) and rolling speed (v , m•s⁻¹), depending on different work roll materials, expressed as:

$$\mu = 1.05 - 0.0005T - 0.056v \text{ for steel work rolls} \quad (7)$$

$$\mu = 0.94 - 0.0005T - 0.056v \text{ for double poured and cast work rolls} \quad (8)$$

Table 2 The calculated COF values obtained under different rolling and lubrication conditions

Lubricant	Temperature/°C	Rolling reduction	Rolling speed/ m•s ⁻¹	Calculated COF	
Water	1050	0.111	0.12	0.34±0.005	
	1050	0.111	0.36	0.28±0.005	
	1050	0.111	0.6	0.27±0.005	
	1050	0.204	0.12	0.25±0	
	1050	0.204	0.36	0.22±0.005	
	1050	0.204	0.6	0.21±0.005	
	1050	0.296	0.12	0.19±0.005	
	1050	0.296	0.36	0.18±0.005	
	1050	0.296	0.6	0.17±0.005	
	4% TiO ₂	1050	0.111	0.12	0.28±0.005
		1050	0.111	0.36	0.27±0
		1050	0.111	0.6	0.26±0.005
		1050	0.204	0.12	0.23±0
		1050	0.204	0.36	0.21±0.005
1050		0.204	0.6	0.19±0	
1050		0.296	0.12	0.18±0	
1050		0.296	0.36	0.175±0.0025	
1050		0.296	0.6	0.165±0	

$$\mu = 0.82 - 0.0005T - 0.056v \text{ for ground work rolls} \quad (9)$$

These equations predict that the COF decreases with the increased workpiece temperature or rolling speed. It is noted that the effect of rolling reduction is not included in Eqs. (7)–(9), nor is that of lubrication. In this work, the improved COF models for both water and 4% TiO₂ lubricant were obtained via linear regression using the data listed in Table 2, written as:

$$\mu_{\text{water}} = 0.395 - 0.631\varepsilon' - 0.09v (R^2 = 0.926) \quad (10)$$

$$\mu_{4\% \text{TiO}_2} = 0.343 - 0.523\varepsilon' - 0.052v (R^2 = 0.956) \quad (11)$$

where μ is the COF during steady-state hot rolling of 304 stainless steel; ε' is the rolling reduction, and v is the rolling speed (m•s⁻¹). As the rolling temperature remains unchanged at 1050 °C, its effect is not included in Eqs. (10) and (11). The correlation coefficients (R^2) of these equations for pure water and 4% TiO₂ lubricant are 0.926 and 0.962, respectively. The improved COF model appears more accurate with the lubricant than pure water.

Figure 7 a and b compare the calculated COF values with those predicted by the improved COF models for water and the lubricant, respectively. In both cases, the results obtained from the COF models agree well with those obtained from the calculation, indicating high accuracy and reliability of the models. In addition to this, the agreement for lubricant case appears better than pure water.

4 Discussion

4.1 Effects of rolling reduction, speed and lubrication on mill load and friction

When using water-based nanolubricants for hot steel rolling, the key factors that affect mill load, i.e. force and torque, include rolling reduction, temperature, speed and lubrication, among which rolling reduction has the most significant effect, and lubrication has the least [48]. As can be seen in Figs. 1 and 2, when the rolling reduction is increased, the rolling force increases significantly. Two competing mechanisms are associated with the rolling process. The increase in rolling reduction raises the strain and the strain rate, which in turn raises the resistance of the steel to deformation, thus leading to an increased rolling force. On the other hand, the increasing reduction results in more plastic work during rolling. This generates more deformation heat and hence a higher temperature on the steel surface, which produces a lower rolling force. Overall, the effect of increased deformation resistance overwhelms that of increased deformation heat, thereby causing a rise in rolling force.

In this study, the entry temperature (1050 °C) remains unchanged for all the rolling tests. Therefore, rolling speed becomes the second important factor that affects mill load. There exist several competing mechanisms that can interpret the speed effect. First, the strain rate rises markedly with the increased rolling speed (see Fig. 3), leading to a higher resistance from the workpiece to deformation and thus an

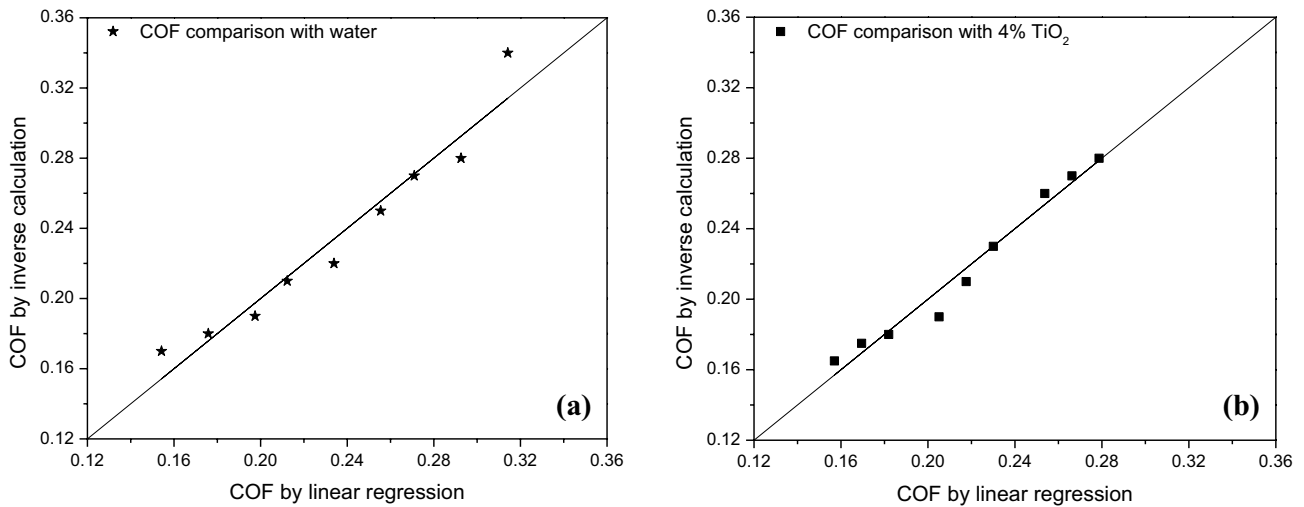


Fig. 7 The COF values obtained from the inverse calculation versus those from the linear regression for **a** water and **b** 4% TiO₂ lubricant

increase in rolling force. Second, rolling speed affects the effective quantity of lubricants in the contact zone. In a faster rolling test, more lubricants can be dragged into the contact zone by the moving surfaces of work rolls. This lowers the COF between the work roll and the workpiece, which contributes to a decreased rolling force. Third, a higher rolling speed corresponds to a less temperature drop during rolling, which should help decrease the rolling force to some extent. Figures 2 and 3 show that an increased speed results in an increased force, suggesting that the strain rate effect overwhelms those caused by lubricant and workpiece temperature. Previous research also supports that the effect of strain rate on steel's resistance to deformation is more significant, particularly at higher rolling temperatures [49], such as the case of 1050 °C in our study.

The 4% TiO₂ lubricant produces much lower mill loads than water, which is particularly true when relatively low rolling reductions and relatively low rolling speeds are employed, as shown in Figs. 2 and 4. This may be because with a higher reduction TiO₂ NPs are more difficult to enter the contact zone as the extreme pressure property of the lubricant becomes poorer. Moreover, the NPs tend to agglomerate with the increase in reduction, which further weakens the lubrication effect. The results shown in Fig. 8 support these derivations. As can be seen in Fig. 8a3, b3, c3, the EDS mappings demonstrate that the effective quantity of TiO₂ NPs remained on the rolled steel surface is inclined to decrease with the increased reduction. Correspondingly, the TiO₂ NPs presented in Fig. 8a4, b4, c4 appear coarser. The ball-bearing effect of the NPs is exemplified in Fig. 8a2, where individual TiO₂ NPs spread over the steel surface rolled with ~10% reduction. In contrast, as shown in Fig. 8c2, when the reduction is increased to ~30%, TiO₂ clusters are found on the rolled steel surface, indicating

agglomeration of NPs. More and smaller TiO₂ NPs in the contact zone actually help lower mill load to a greater extent [26]. When rolling at relatively high speeds, the increased speed significantly enhances the resistance to material deformation, thus leading to a higher mill load for both water and lubricant. As a result, the load difference caused by water and the lubricant becomes less distinct. The NPs can also affect rolling through mending the surface defects, as shown in Fig. 8a1, b1, c1.

Introducing lubricants into the contact zone between the work roll and the workpiece increases the complexity of friction. As discussed earlier, the increase in rolling speed allows more lubricants to enter the contact zone, and hence a drop in COF. As can be derived from Eq. (11), an increasing reduction also leads to a drop in COF. When the reduction is increased, the experienced pressure of the lubricant increases, so does the viscosity [50]. The increased viscosity prompts a decreased COF. On the other hand, the risen interfacial temperature is always associated with the increased reduction, which somewhat lowers the viscosity of lubricant and thus leads to a higher COF. Figure 8 demonstrates that fewer and larger NPs are present in the contact zone when rolled under a higher reduction, which therefore aggravates the friction between the work roll and the workpiece. In this study, pressure appears to have more dominant effect on reducing the COF than other factors.

4.2 Lubrication mechanism

To understand the possible lubrication mechanisms involved in the hot rolling of 304 stainless steel, it is necessary to first determine the lubrication regime. According to the well-known Stribeck curve, there are three types of lubrication regimes, including boundary lubrication, mixed lubrication

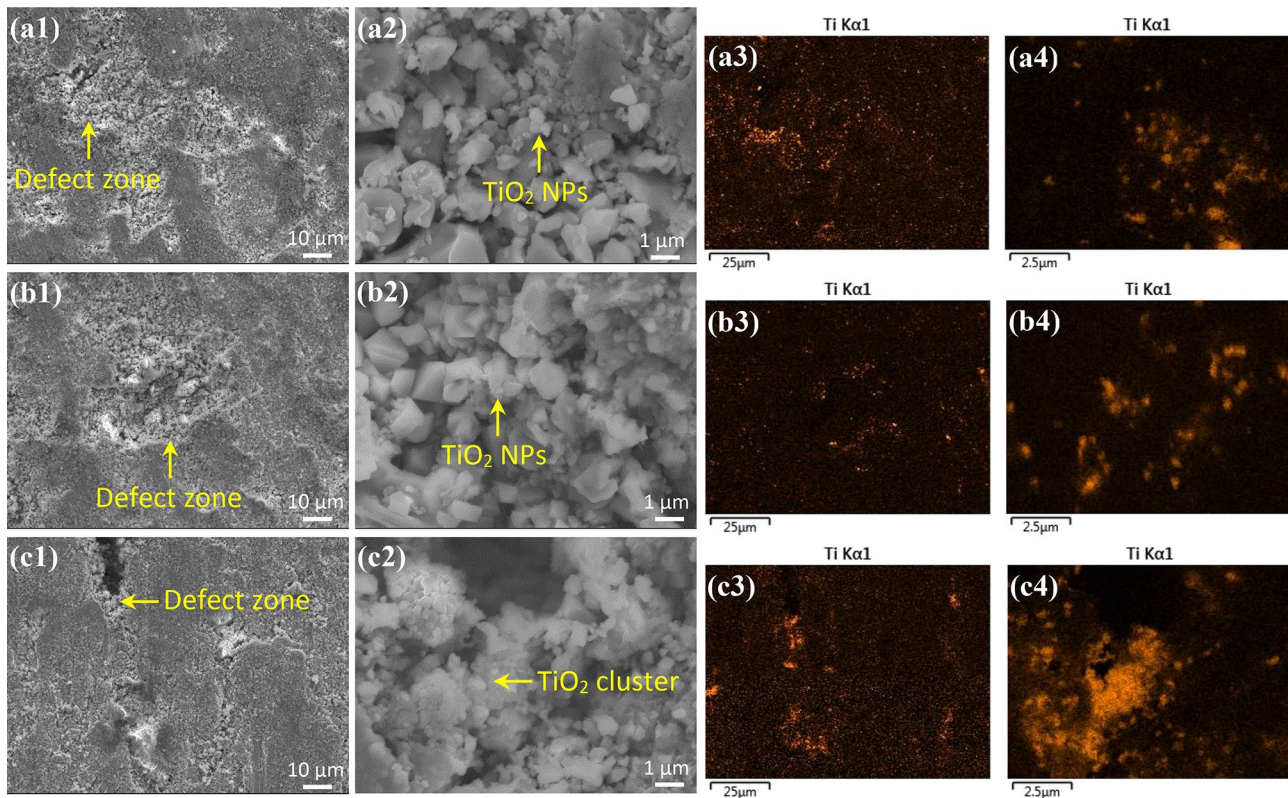


Fig. 8 SEM images and EDS mappings of the steel surfaces after rolling with 4% TiO_2 lubricant under (a1–a4) ~10%, (b1–b4) ~20% and (c1–c4) ~30% reductions. (a1), (b1) and (c1) corresponds to (a3),

(b3) and (c3), respectively, at 1000× magnification; (a2), (b2) and (c2) corresponds to (a4), (b4) and (c4), respectively, at 10,000× magnification. The rolling speed is fixed at $0.36 \text{ m}\cdot\text{s}^{-1}$

and hydrodynamic lubrication [51]. It is possible to determine the lubrication regime during rolling by comparing the thickness of the lubricant film (h_{\min}) and the combined asperity heights (R'_q) of the work roll and the workpiece [52]. The ratio (λ) and R'_q are defined as:

$$\lambda = h_{\min}/R'_q \quad (12)$$

$$R'_q = \sqrt{R_{q1}^2 + R_{q2}^2} \quad (13)$$

where R_{q1} and R_{q2} are the surface roughness values (R_q) of the work roll and workpiece, respectively. As reported elsewhere [53], boundary lubrication is present when λ is less than 1; mixed lubrication prevails when $1 \leq \lambda \leq 3$, while hydrodynamic lubrication occurs at a λ value over 3.

The lubricant film thickness (h_s) at the inlet of rolling mill can be calculated using the formula derived by Wilson and Walowit [54], expressed as:

$$h_s = \frac{3\eta_0\gamma(v_{\text{entry}} + v_{\text{roll}})r'}{l[1 - \exp(-\gamma\sigma_y)]} \quad (14)$$

where η_0 is the dynamic viscosity of lubricant under ambient pressure ($\text{Pa}\cdot\text{s}$); γ is the pressure-viscosity coefficient (Pa^{-1}) which links the variation of viscosity with a change in pressure; v_{entry} and v_{roll} are the strip entry speed and roll surface speed, respectively, both in $\text{m}\cdot\text{s}^{-1}$. They are assumed to be the same in this study. l in Eq. (14) is the contact length, defined as $l = \sqrt{r \cdot \Delta h}$, where r is the radius of work roll, and Δh is the reduction of thickness. σ_y is the yield strength of the strip at ambient temperature. r' is the deformed roll radius that can be calculated with the knowledge of the Poisson's ratio and Young's modulus of the work roll [55]. It should be noted that Eq. (14) was proposed for cold rolling of metals. Some parameters such as η_0 and σ_y in this equation should be corrected to high-pressure dynamic viscosity of the lubricant and high-temperature yield strength of the strip, respectively. For the hot steel rolling conditions, the actual yield strength of the strip at 1050°C under varying strain rates can be estimated using Eq. (6), in which the strain is selected at 0.2%.

In fact, the viscosity of lubricant during hot steel rolling is not constant, but rather a function of temperature and pressure [56]. Figure 9 shows the results of dynamic viscosity measurement at 80°C under increasing pressures up to 15 MPa. It can

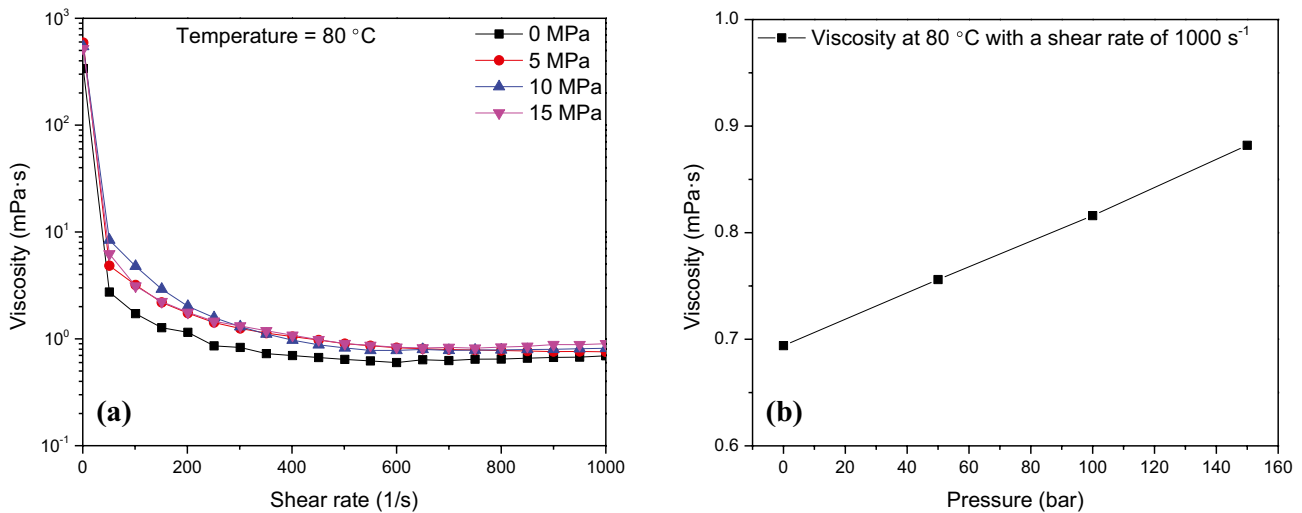


Fig. 9 Viscosity values of 4% TiO₂ lubricant measured at 80 °C under pressures of 0, 5, 10 and 15 MPa: **a** viscosities plotted against shear rate; **b** the viscosities averaged using the data from the stable stages in **a** plotted against pressure

be seen in Fig. 9a that the viscosity of lubricant decreases continuously within 600 s⁻¹ and then remains stable as the strain rate is increased to 1000 s⁻¹, indicating that the lubricant is a non-Newtonian fluid. For calculating the lubricant film thickness in this work, the viscosity values at the stable stages are averaged, as shown in Fig. 9b. It is found that the viscosity rises with the increased pressure. The pressure-viscosity coefficient (γ) can be determined using the data in Fig. 9b, which aims to predict the viscosities of a lubricant under unmeasured high contact pressures generated in hot steel rolling. The pressure-viscosity coefficient (γ) is defined as:

$$a_p = \exp(\gamma(P - P_{ref})) \tag{15}$$

$$a_p = \eta_p / \eta_{p_{ref}} \tag{16}$$

where a_p is the pressure shift factor; η_p and $\eta_{p_{ref}}$ are lubricant viscosities under a selected pressure (P) and a reference

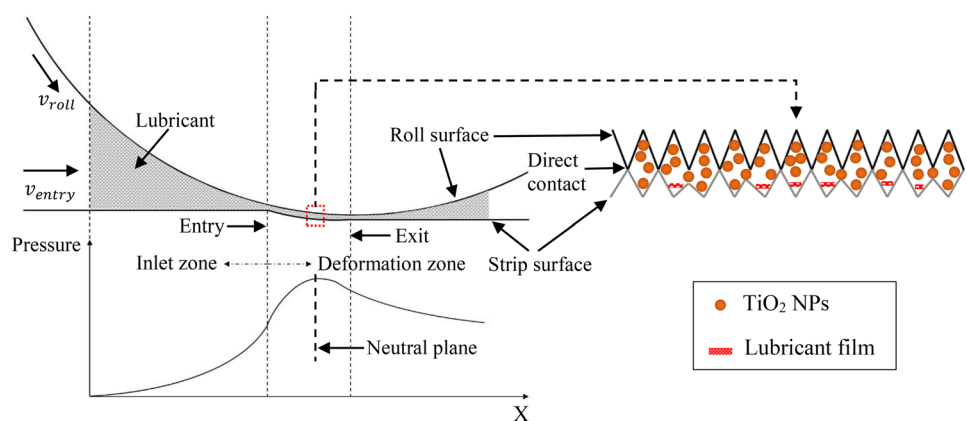
pressure (P_{ref}), respectively, according to the viscosity-pressure data in Fig. 9b. The calculation result shows that the pressure-viscosity coefficient (γ) is 0.0153 MPa⁻¹.

In hot steel rolling, the contact pressure gradually increases from the entry to the neutral point [57]. The average contact pressure (\bar{P}) during rolling can be used to approximately represent the pressure applied on the lubricant. \bar{P} is calculated as:

$$\bar{P} = \frac{F}{\bar{B}\sqrt{r \cdot \Delta h}} \tag{17}$$

where F is the rolling force; \bar{B} is the average width of the workpiece before and after rolling; r is the radius of work roll and Δh is the thickness reduction. From Eqs. (12)–(17), the calculated lubricant film thickness varies from 3 to 25 nm in all the rolling tests using 4% TiO₂ lubricant, which is far below the size of TiO₂ NP and the surface roughness of workpiece. The corresponding values of λ are

Fig. 10 Schematic illustration of the lubrication mechanisms using water-based lubricant containing TiO₂ NPs for hot rolling of 304 stainless steel



in the range of 0.003–0.024, indicating a boundary lubrication regime occurred in the hot rolling of 304 stainless steel. This implies that the lubricant film is insufficiently thick to prevent the work roll and the workpiece from direct contact, while the TiO₂ NPs indeed play a more dominant role in lubrication effectiveness. In view of this, the lubrication mechanisms involved are ascribed to three components. First, there exist substantial metal to metal contacts via the surface asperities of work roll and workpiece, which exacerbates the friction in between. Second, the TiO₂ NPs act as ball bearings that can roll in the contact zone, contributing to the decrease in friction. Meanwhile, the NPs can be pressed into the surface defects of the strip, playing a mending effect. Third, some thin lubricant films are likely to be entrapped in the surface pockets, and therefore relieve the direct metal to metal contact to some extent. These lubrication mechanisms are summarised illustratively in Fig. 10.

5 Conclusions

In this study, the hot rolling of 304 stainless steel was carried out at 1050 °C under rolling reductions of 10–30% and rolling speeds of 0.12–0.6 m•s⁻¹ using both water and water-based lubricant containing 4% TiO₂ NPs. The influence of water-based nanolubrication on rolling force, torque, power and contact friction was systematically investigated, and the lubrication mechanisms were proposed. The main conclusions are drawn as follows:

- The rolling force has a linear relationship with the rolling reduction or strain rate. The rolling force with 4% TiO₂ nanolubricant is 6.1% lower than that with pure water lubrication for the ~10% reduction with the rolling speed less than 0.36 m•s⁻¹.
- The rolling torque and power obtained using pure water lubrication can be decreased by over 5% in all the rolling tests when using 4% TiO₂ nanolubricant.
- The lubrication becomes less effective at relatively high rolling reduction and speed, in terms of load reduction.
- Improved COF models are developed with the inclusion of rolling reduction and speed. The models exhibit satisfactory accuracy in the prediction of the COF in the steady-state hot rolling of 304 stainless steel.
- A boundary lubrication regime is formed during the hot steel rolling, and the excellent lubricity of the nanolubricant is ascribed to the ball bearing and mending effects of TiO₂ NPs, as well as the formation of thin lubricant films.

Acknowledgements The authors appreciate the financial support from the Baosteel-Australia Joint Research and Development Centre under

the project of BA17004, and the Australian Research Council under the Linkage Project Program of LP150100591. The authors would like to thank all the technical staff in the workshop of the SMART Infrastructure Facility at the University of Wollongong for their great support in sample preparation and hot rolling of steels.

Author contribution Hui Wu: conceptualization, methodology, data collection and analysis, investigation, writing—original draft preparation, reviewing and editing; Dongbin Wei: methodology, data collection and analysis, writing—reviewing and editing; Ay Ching Hee: methodology, data collection and analysis, writing—reviewing and editing; Shuiquan Huang: material preparation, data analysis, writing—reviewing and editing; Zhao Xing: methodology, material preparation, data analysis; Sihai Jiao: conceptualization, supervision, methodology, data analysis, investigation; Han Huang: conceptualization, supervision, methodology, data analysis, investigation, writing—reviewing and editing; Zhengyi Jiang: conceptualization, supervision, methodology, data analysis, investigation, writing—reviewing and editing.

Funding Open Access funding enabled and organized by CAUL and its Member Institutions. This work was financially supported by the Baosteel-Australia Joint Research and Development Centre under the project of BA17004, and the Australian Research Council under the Linkage Project Program of LP150100591.

Declarations

Conflict of interest The authors declare that they have no known competing financial interest or personal relationships that could have appeared to influence the work reported in this paper.

Open Access This article is licensed under a Creative Commons Attribution 4.0 International License, which permits use, sharing, adaptation, distribution and reproduction in any medium or format, as long as you give appropriate credit to the original author(s) and the source, provide a link to the Creative Commons licence, and indicate if changes were made. The images or other third party material in this article are included in the article's Creative Commons licence, unless indicated otherwise in a credit line to the material. If material is not included in the article's Creative Commons licence and your intended use is not permitted by statutory regulation or exceeds the permitted use, you will need to obtain permission directly from the copyright holder. To view a copy of this licence, visit <http://creativecommons.org/licenses/by/4.0/>.

References

1. Zhao J, Jiang Z (2018) Thermomechanical processing of advanced high strength steels. *Prog Mater Sci* 94:174–242
2. Jiang ZY, Tang J, Sun W, Tieu AK, Wei D (2010) Analysis of tribological feature of the oxide scale in hot strip rolling. *Tribol Int* 43(8):1339–1345
3. Cheng X, Jiang Z, Wei D, Zhao J, Monaghan BJ, Longbottom RJ, Jiang L (2014) Characteristics of oxide scale formed on ferritic stainless steels in simulated reheating atmosphere. *Surf Coat Technol* 258:257–267
4. Ha DJ, Sung HK, Lee S, Lee JS, Lee YD (2009) Analysis and prevention of sticking occurring during hot rolling of ferritic stainless steel. *Mater Sci Eng A* 507(1–2):66–73
5. Yu Y, Lenard JG (2002) Estimating the resistance to deformation of the layer of scale during hot rolling of carbon steel strips. *J Mater Process Technol* 121(1):60–68

6. Azushima A, Xue WD, Yoshida Y (2009) Influence of lubricant factors on coefficient of friction and clarification of lubrication mechanism in hot rolling. *ISIJ Int* 49(6):868–873
7. Shirizly A, Lenard JG (2000) The effect of lubrication on mill loads during hot rolling of low carbon steel strips. *J Mater Process Technol* 97(1–3):61–68
8. Müller M, Prinz K, Steinboeck A, Schausberger F, Kugi A (2020) Adaptive feedforward thickness control in hot strip rolling with oil lubrication. *Control Eng Pract* 103:104584
9. Li YL, Cao JG, Kong N, Wen D, Ma HH, Zhou YS (2017) The effects of lubrication on profile and flatness control during ASR hot strip rolling. *Int J Adv Manuf Technol* 91(5–8):2725–2732
10. Azushima A, Xue WD, Yoshida Y (2007) Lubrication mechanism in hot rolling by newly developed simulation testing machine. *CIRP Ann-Manuf Technol* 56(1):297–300
11. Matsuoka S, Morita M, Furukimi O, Obara T (1998) Effect of lubrication condition on recrystallization texture of ultra-low C sheet steel hot-rolled in ferrite region. *ISIJ Int* 38(6):633–639
12. Haus F, German J, Junter GA (2001) Primary biodegradability of mineral base oils in relation to their chemical and physical characteristics. *Chemosphere* 45(6–7):983–990
13. Xia WZ, Zhao JW, Wu H, Zhao XM, Zhang XM, Xu JZ, Jiao SH, Wang XG, Zhou CL, Jiang ZY (2018) Effects of oil-in-water based nanolubricant containing TiO₂ nanoparticles in hot rolling of 304 stainless steel. *J Mater Process Technol* 262:149–156
14. Xia W, Zhao J, Wu H, Jiao S, Zhao X, Zhang X, Xu J, Jiang Z (2018) Analysis of oil-in-water based nanolubricants with varying mass fractions of oil and TiO₂ nanoparticles. *Wear* 396–397:162–171
15. Xia WZ, Zhao JW, Wu H, Jiao SH, Jiang ZY (2017) Effects of oil-in-water based nanolubricant containing TiO₂ nanoparticles on the tribological behaviour of oxidised high-speed steel. *Tribol Int* 110:77–85
16. Huang SQ, Lin WK, Li XL, Fan ZQ, Wu H, Jiang ZY, Huang H (2021) Roughness-dependent tribological characteristics of water-based GO suspensions with ZrO₂ and TiO₂ nanoparticles as additives. *Tribol Int* 161:107073
17. Huang SQ, Li XL, Zhao YT, Sun Q, Huang H (2021) A novel lapping process for single-crystal sapphire using hybrid nanoparticle suspensions. *Int J Mech Sci* 191:106099
18. Huang S, Li X, Mu D, Cui C, Huang H, Huang H (2021) Polishing performance and mechanism of a water-based nanosuspension using diamond particles and GO nanosheets as additives. *Tribol Int* 164:107241
19. Huo MS, Wu H, Xie HB, Zhao JW, Su GQ, Jia FH, Li Z, Lin F, Li SL, Zhang HM, Jiang ZY (2020) Understanding the role of water-based nanolubricants in micro flexible rolling of aluminium. *Tribol Int* 151:106378
20. He AS, Huang SQ, Yun JH, Wu H, Jiang ZY, Stokes J, Jiao SH, Wang LZ, Huang H (2017) Tribological performance and lubrication mechanism of alumina nanoparticle water-based suspensions in ball-on-three-plate testing. *Tribol Lett* 65(2):40
21. He AS, Huang SQ, Yun JH, Jiang ZY, Stokes J, Jiao SH, Wang LZ, Huang H (2017) The pH-dependent structural and tribological behaviour of aqueous graphene oxide suspensions. *Tribol Int* 116:460–469
22. He AS, Huang SQ, Yun JH, Jiang ZY, Stokes JR, Jiao SH, Wang LZ, Huang H (2018) Tribological characteristics of aqueous graphene oxide, graphitic carbon nitride, and their mixed suspensions. *Tribol Lett* 66(1):42
23. Wu H, Jia FH, Li Z, Lin F, Huo MS, Huang SQ, Sayyar S, Jiao SH, Huang H, Jiang ZY (2020) Novel water-based nanolubricant with superior tribological performance in hot steel rolling. *Int J Extreme Manuf* 2(2):025002
24. Wu H, Jiang CY, Zhang JQ, Huang SQ, Wang LZ, Jiao SH, Huang H, Jiang ZY (2019) Oxidation behaviour of steel during hot rolling by using TiO₂-containing water-based nanolubricant. *Oxid Met* 92(3–4):315–335
25. Wu H, Zhao JW, Luo L, Huang SQ, Wang LZ, Zhang SQ, Jiao SH, Huang H, Jiang ZY (2018) Performance evaluation and lubrication mechanism of water-based nanolubricants containing nano-TiO₂ in hot steel rolling. *Lubricants* 6(3):57
26. Wu H, Zhao JW, Xia WZ, Cheng XW, He AS, Yun JH, Wang LZ, Huang H, Jiao SH, Huang L, Zhang SQ, Jiang ZY (2017) Analysis of TiO₂ nano-additive water-based lubricants in hot rolling of microalloyed steel. *J Manuf Processes* 27:26–36
27. Xiong S, Liang D, Wu H, Lin W, Chen J, Zhang B (2021) Preparation, characterization, tribological and lubrication performances of Eu doped CaWO₄ nanoparticle as anti-wear additive in water-soluble fluid for steel strip during hot rolling. *Appl Surf Sci* 539:148090
28. He JQ, Sun JL, Meng YA, Yang FL, Tang HJ (2021) MoS₂-Al₂O₃ nanofluid-induced microstructure evolution and corrosion resistance enhancement of hot-rolled steel surface. *J Mater Sci* 56(31):17805–17823
29. He J, Sun J, Meng Y, Pei Y (2020) Superior lubrication performance of MoS₂-Al₂O₃ composite nanofluid in strips hot rolling. *J Manuf Processes* 57:312–323
30. Huang SQ, Wu H, Jiang ZY, Huang H (2021) Water-based nanosuspensions: formulation, tribological property, lubrication mechanism, and applications. *J Manuf Processes* 71:625–644
31. Wu H, Jia FH, Zhao JW, Huang SQ, Wang LZ, Jiao SH, Huang H, Jiang ZY (2019) Effect of water-based nanolubricant containing nano-TiO₂ on friction and wear behaviour of chrome steel at ambient and elevated temperatures. *Wear* 426:792–804
32. Wu H, Zhao JW, Cheng XW, Xia WZ, He AS, Yun JH, Huang SQ, Wang LZ, Huang H, Jiao SH, Jiang ZY (2018) Friction and wear characteristics of TiO₂ nano-additive water-based lubricant on ferritic stainless steel. *Tribol Int* 117:24–38
33. Wu H, Zhao JW, Xia WZ, Cheng XW, He AS, Yun JH, Wang LZ, Huang H, Jiao SH, Huang L, Zhang SQ, Jiang ZY (2017) A study of the tribological behaviour of TiO₂ nano-additive water-based lubricants. *Tribol Int* 109:398–408
34. Morshed A, Wu H, Jiang ZY (2021) A comprehensive review of water-based nanolubricants. *Lubricants* 9(9):89
35. Wu H, Kamali H, Huo MS, Lin F, Huang SQ, Huang H, Jiao SH, Xing Z, Jiang ZY (2020) Eco-friendly water-based nanolubricants for industrial-scale hot steel rolling. *Lubricants* 8(11):96
36. Wei DB, Huang JX, Zhang AW, Jiang ZY, Tieu AK, Shi X, Jiao SH, Qu XY (2009) Study on the oxidation of stainless steels 304 and 304L in humid air and the friction during hot rolling. *Wear* 267(9–10):1741–1745
37. Wei DB, Huang JX, Zhang AW, Jiang ZY, Tieu AK, Shi X, Jiao SH (2011) The effect of oxide scale of stainless steels on friction and surface roughness in hot rolling. *Wear* 271(9–10):2417–2425
38. Jin W, Piereder D, Lenard JG (2002) A study of the coefficient of friction during hot rolling of a ferritic stainless steel. *Lubr Eng* 58(11):29–37
39. Lenard JG, Barbulovic-Nad L (2002) The coefficient of friction during hot rolling of low carbon steel strips. *J Tribol-Trans ASME* 124(4):840–845
40. Hanaor DAH, Assadi MHN, Li S, Yu A, Sorrell CC (2012) Ab initio study of phase stability in doped TiO₂. *Comput Mech* 50(2):185–194
41. Greenwood NN, Earnshaw A (2012) *Chemistry of the Elements*, Elsevier
42. Alexander JM, Brewer RC, Rowe GW (1987) *Manufacturing technology*. Vol. 2. Engineering Processes, Ellis Horwood, Market Cross House, Cooper Street, Chichester, West Sussex PO 19 1EB, UK, 1987
43. Orowan E (1943) The calculation of roll pressure in hot and cold flat rolling. *Proc Inst Mech Eng* 150(1):140–167
44. Cheng X, Jiang Z, Zhao J, Wei D, Hao L, Peng J, Luo M, Ma L, Luo S, Jiang L (2015) Investigation of oxide scale on ferritic

- stainless steel B445J1M and its tribological effect in hot rolling. *Wear* 338–339:178–188
45. Cheng X, Jiang Z, Wei D, Hao L, Zhao J, Jiang L (2015) Oxide scale characterization of ferritic stainless steel and its deformation and friction in hot rolling. *Tribol Int* 84:61–70
 46. Ginzburg VB (2020) *Metallurgical design of flat rolled steels*, CRC press
 47. Pietrzyk M, Cser L, Lenard J (1999) *Mathematical and physical simulation of the properties of hot rolled products*, Elsevier
 48. Wu H, Huang SQ, Xing Z, Jiao SH, Huang H, Jiang ZY (2022) The effect of water-based nanolubrication on friction during hot steel rolling, (Under review)
 49. Lin YC, Chen MS, Zhong J (2008) Effect of temperature and strain rate on the compressive deformation behavior of 42CrMo steel. *J Mater Process Technol* 205(1–3):308–315
 50. Pawelski O, Rasp W, Draese S (1994) Influence of hydrodynamic lubricant entrainment on friction effects in cold-rolling. *Steel Res* 65(11):488–493
 51. Schmid SR, Saha PK, Wang J, Schmitz T (2020) Developments in tribology of manufacturing processes, *J Manuf Sci Eng* 142(11)
 52. Lenard JG (2000) Tribology in Metal rolling keynote presentation forming group F, *CIRP Ann-Manuf Technol* 49(2):567–590
 53. Xie H, Dang S, Jiang B, Xiang L, Zhou S, Sheng H, Yang T, Pan F (2019) Tribological performances of SiO₂/graphene combinations as water-based lubricant additives for magnesium alloy rolling. *Appl Surf Sci* 475:847–856
 54. Wilson W (1971) An isothermal hydrodynamic lubrication theory for strip rolling with front and back tension. *Tribology Convention* 1971:169–172
 55. Xie H, Manabe K-I, Furushima T, Tada K, Jiang Z (2016) Lubrication characterisation analysis of stainless steel foil during micro rolling. *Int J Adv Manuf Technol* 82(1):65–73
 56. McConnell C, Lenard JG (2000) Friction in cold rolling of a low carbon steel with lubricants. *J Mater Process Technol* 99(1–3):86–93
 57. Sheu S (2013) Tribology in hot rolling of metal. In: Wang QJ, Chung Y-W (eds) *Encyclopedia of Tribology*. Springer, US, Boston, MA, pp 3830–3837

Publisher's Note Springer Nature remains neutral with regard to jurisdictional claims in published maps and institutional affiliations.